VOL. 53 NO. 3, MAR. 2000 THE JOURNAL OF ANTIBIOTICS pp. 269 — 275

Structures of ADP-Ribosylated Rifampicin and Its Metabolite: Intermediates of Rifampicin-ribosylation by *Mycobacterium smegmatis* DSM43756

NAOKO MORISAKI and YUICHI HASHIMOTO*

Institute of Molecular and Cellular Biosciences, The University of Tokyo,
1-1-1 Yayoi, Bunkyo-ku, Tokyo 113-0032, Japan

KAZUO FURIHATA

Division of Agriculture and Agricultural Life Sciences, The University of Tokyo,
1-1-1 Yayoi, Bunkyo-ku, Tokyo 113-8657, Japan

TAMAE IMAI, KAYO WATANABE, YUZURU MIKAMI and KATSUKIYO YAZAWA

Research Center for Pathogenic Fungi and Microbial Toxicoses, Chiba University,
1-8-1 Inohana, Chuo-ku, Chiba 260-8673, Japan

AKIKAZU ANDO and YOSHIHO NAGATA

Department of Biotechnology, Graduate School of Science and Technology, Chiba University,
1-33 Yayoi, Inage-ku, Chiba 271-8510, Japan

ERIC R. DABBS

Molecular and Cell Biology Department, University of the Witwatersrand,
Johannesburg, P O WITS 2050, South Africa

(Received for publication November 11, 1999)

23-(*O*-ADP-Ribosyl)rifampicin [RIP-TAs (**3**, Na^+ form), RIP-TAf (**4**, H^+ form)] was obtained as an intermediate in the conversion process of rifampicin (**1**) to RIP-Mb (**2**) that is mediated by cell homogenates of *Mycobacterium smegmatis* DSM43756 or of *Escherichia coli* carrying a mycobacterial mono(ADP-ribosyl) transferase gene, in the presence of NADH. 23-[*O*-(5′-Phosphoribosyl)]rifampicin (**5**, RIP-TAp) was also obtained by the reaction of rifampicin with NADH in the presence of a homogenate of *M. smegmatis*. The structures of **3**, **4**, and **5** were determined by means of MS and NMR analyses.

The semisynthetic antibiotic rifampicin (**1**) is an important chemotherapeutic agent used to treat tuberculosis, leprosy, and other infectious diseases.[1~3] It acts by inhibiting bacterial DNA-dependent RNA polymerase. A resistance mechanism involving alteration in the β-subunit of the enzyme has been reported for *Mycobacterium tuberculosis* and *M. leprae*.[4] Another mechanism of resistance is conversion of rifampicin to its inactivated form or degradation. We found that rifampicin is inactivated by glucosylation at 23-OH or phosphorylation at 21-OH, or by decomposition in *Nocardia* and *Bacillus* species.[5~9]

During studies on fast-growing mycobacterial strains,[10,11] we found that *Mycobacterium smegmatis* DSM43756 inactivates rifampicin by the formation of 3-formyl-23-[*O*-(α-D-ribofuranosyl)]rifamycin SV (RIP-Ma) and 23-[*O*-(α-D-ribofuranosyl)]rifampicin (RIP-Mb, **2**).[12,13] In order to study the inactivation by ribosylation at the 23-OH group of rifampicin and to identify the origin of the ribose moiety, the gene of *M. smegmatis* DSM43756 responsible for the inactivation was cloned and expressed in *Escherichia coli* (*E. coli* #49).[14] In the presence of NADH, cell homogenates of the transformant converted rifampicin to a new inactivated compound, 23-(*O*-ADP-

Fig. 1. Structures of rifampicin (**1**), RIP-Mb (**2**), RIP-TAs (**3**), RIP-TAf (**4**) and RIP-TAp (**5**).

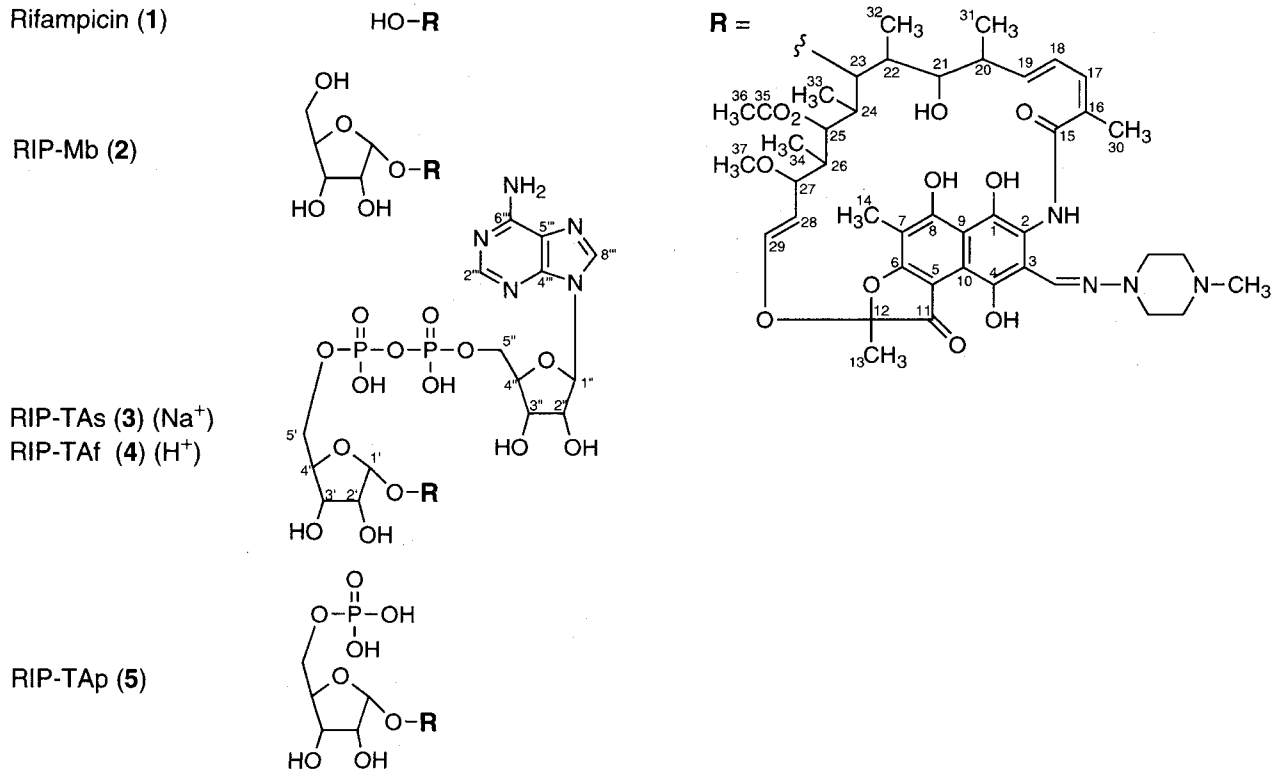

ribosyl)rifampicin (RIP-TAs, **3**), indicating that the gene encodes a mono(ADP-ribosyl)transferase.[15] In the presence of NADH, cell homogenates of *M. smegmatis* DSM43756 converted rifampicin to RIP-Mb (**2**), RIP-TAs (**3**), and 23-[*O*-(5′-phosphoribosyl)]rifampicin (RIP-TAp, **5**).[16] A study on the conversion of RIP-TAs (**3**) to RIP-Mb (**2**) with cell homogenates of *M. smegmatis* DSM43756 showed that the ribose moiety in RIP-TAb (**2**) was derived from NADH.[16] Here we present details of the structural determination of RIP-TAs (**3**, Na^+ salt), RIP-TAf (**4**, free phosphate form of RIP-TAs), and RIP-TAp (**5**) (Fig. 1).

Experimental

^1H, ^{13}C and ^{31}P NMR spectra were measured in CD_3OD at 25°C on a JEOL ALPHA-500 NMR spectrometer at 500 MHz (spectral width 5,000 Hz, 32,000 data points), 125 MHz (spectral width 32,000 Hz, 32,000 data points) and 202.35 MHz (spectral width 10,000 Hz, 16,000 data points), respectively. NMR spectra of RIP-TAp (**5**) were measured with a Nalorac 3 mm i.d. tunable probe head. Chemical shifts in ^1H and ^{13}C NMR were recorded in δ units relative to methanol (δ_H=3.30 ppm and δ_C=49.0 ppm, respectively) and those in ^{31}P NMR were recorded relative to external potassium phosphate (δ_P=0). ^1H and ^{13}C NMR signals were assigned on the basis of COSY, pulse-field gradient heteronuclear multi quantum coherence (PFG-HMQC) and pulse-field gradient heteronuclear multiple-bond correlation (PFG-HMBC) experiments. Positive and negative ion FAB MS and HRFAB MS were measured on a JEOL JMS-HX110 double-focusing mass spectrometer of EBE arrangement with a JMS-DA7000 data system. Ion acceleration voltage was 10 kV, and the fast-atom xenon gas was accelerated at a voltage of 6 kV. Glycerol was used as the matrix. Polyethyleneglycol 1000 and 1540 was used as standard compounds for HRFAB mass calibration.

RIP-TAs (3) and RIP-TAf (4)

Rifampicin (60 mg) and NADH (100 mg) were incubated with cell homogenates of *E. coli* #49 at 37°C for 3 hours.[15] The reaction mixture was centrifuged, and the supernatant was freeze-dried. The dried mixture was extracted with

Table 1. Molecular formulae, molecular weights and mass spectral data of RIP-TAs (**3**), RIP-TAf (**4**) and RIP-TAp (**5**).

	Molecular formula & molecular weight	Positive ion FAB-MS	Negative ion FAB-MS	HRFAB-MS
RIP-TAs (**3**)	$C_{58}H_{79}N_9O_{25}P_2$ 1363	*m/z* 1408 (M+2Na-H) 1430 (M+3Na-2H) 1452 (M+4Na-3H)	*m/z* 1384 (M+Na-2H) 1406 (M+2Na-3H)	Calcd. for $C_{58}H_{77}N_9O_{25}P_2Na_3$ (M+3Na-2H) 1430.4199 Found 1430.4119
RIP-TAf (**4**)	$C_{58}H_{79}N_9O_{25}P_2$ 1363	*m/z* 1364 (M+H) 1386 (M+Na)	*m/z* 1362 (M-H)	Calcd. for $C_{58}H_{78}N_9O_{25}P_2Na_2$ (M+2Na-H) 1408.4380 Found 1408.4301*
RIP-TAp (**5**)	$C_{48}H_{67}N_4O_{19}P$ 1034	*m/z* 1035 (M+H) 1057 (M+Na) 1079 (M+2Na-H)	*m/z* 1033 (M-H) 1055 (M+Na-2H)	Calcd. for $C_{48}H_{67}N_4O_{19}PNa$ (M+Na) 1057.4035 Found 1057.4010

* Analyzed after the addition of NaCl.

8 ml of methanol, and the extracts were chromatographed on a Sephadex LH-20 column (28 mm i.d.×290 mm) with methanol. Two colored compounds were obtained: RIP-TAf (**4**, 29 mg) and RIP-TAs (**3**,[15] 43 mg), in order of elution from the column.

Compound **4** was only slightly soluble in methanol, whereas **3** was soluble. The Rf values of **3** and **4** on a reversed-phase TLC plate (KF18F, J. T. Baker, Inc.) developed with 0.2 M NaCl : DMSO : CH_3CN=4 : 1.5 : 4 were both 0.8. In reversed-phase HPLC on a Lichrospher 100, PR-18(e) column (Cica-Merck, 4.6 mm i.d.×150 mm) (eluent: 38 % CH_3CN-0.05 % TFA, flow rate: 1 ml/minute, detection: UV 270 nm), **3** and **4** had the same retention time (7.3 minutes). FAB MS and NMR data for RIP-TAs (**3**) and RIP-TAf (**4**) are listed in Tables 1~3.[17]

RIP-TAp (**5**)

Rifampicin (15 mg) and NADH (25 mg) were incubated with cell homogenates of *M. smegmatis* DSM43756 at 33° for 65 hours.[16] After lyophilization, the dried mixture containing rifampicin (**1**), RIP-TAs (**3**) and RIP-TAp (**5**) was extracted with methanol. RIP-TAp (**5**) was purified by silica gel column chromatography followed by reversed-phase TLC, and Sephadex LH20 column chromatography.[16] This preparation was repeated three times, and from 45 mg of rifampicin, *ca.* 2 mg of purified RIP-TAp was obtained. FAB MS, ^1H and ^{13}C NMR data of **5** are listed in Tables 1~3.

Results and Discussion

The structures of RIP-TAs (**3**), RIP-TAf (**4**), and RIP-TAp (**5**) were determined by comparison of the spectroscopic data with those of rifampicin (**1**)[6] and RIP-Mb (**2**)[13].

Positive and negative ion FAB MS data of RIP-TAs (**3**) indicated the molecular weight to be 1363, and the molecular formula was determined by HRFAB MS to be $C_{58}H_{79}N_9O_{25}P_2$ (Table 1). Taking into account that NADH was essential for the formation of RIP-TAs (**3**) from rifampicin (**1**) with *E. coli* #49 homogenates, the molecular formula of **3** was in accord with that expected for ADP-ribosylated rifampicin, or the 5′-adenosine diphosphate of RIP-Mb (**2**), and this was confirmed by the NMR data (Tables 2 and 3). The presence of adenosine phosphate was indicated by signals at δ_C 89.2 (C-1″), 76.4 (C-2″), 71.8 (C-3″), 85.5 (C-4″), 66.3 (C-5″), 153.8 (C-2‴), 150.7 (C-4‴), 120.1 (C-5‴), 157.3 (C-6‴) and 141.3 (C-8‴) ppm, and at δ_H 6.08 (H-1″), 4.60 (H-2″), 4.45 (H-3″), 4.23 (H-4″), 4.20 (H-5″), 8.17 (H-2‴) and 8.54 (H-8‴) ppm.[18,19] Phosphorylation of 5′-OH and 5″-OH was confirmed by long-range couplings of C-4′, C-4″, C-5′ and C-5″ with the phosphorus atom; $J_{C\text{-}O\text{-}P}$ of the former two carbons was

Table 2. ^{1}H NMR chemical shifts (δ, ppm), multiplicities and coupling constants (J, Hz) of rifampicin (**1**), RIP-Mb (**2**), RIP-TAs (**3**), RIP-TAf (**4**) and RIP-TAp (**5**) in CD_3OD.

Reference: methanol, δ=3.30 ppm.

Proton	Rifampicin (**1**)[*6]	RIP-Mb (**2**)[*13]	RIP-TAs (**3**)	RIP-TAf (**4**)	RIP-TAp (**5**)
13	1.71 (3H, s)	1.70 (3H, s)	1.68 (3H, s)	1.69 (3H, s)	1.69 (3H, s)
14	2.02 (3H, s)	2.02 (3H, s)[*2]	1.99 (3H, s)	2.00 (3H, s)	2.00 (3H, s)
17	6.35 (1H, br d, 10.5)	6.36 (1H, d,11.0)	6.28 (1H, d,11.0)	6.32 (1H, d,11.0)	6.34 (1H, d,10.5)
18	7.25 (1H, dd, 15.8, 10.5)	7.17 (1H, dd,15.5, 11.0)	6.80 (1H, dd,15.5, 10.0)	7.09 (1H, brdd,15.5, 11.0)	7.07 (1H, dd,16.0, 11.0)
19	6.08 (1H, dd, 15.8, 7.0)	6.10 (1H, dd,15.5, 7.0)	5.95 (1H, dd,15.5, 7.0)	6.00 (1H, dd,15.5, 7.0)	6.06 (1H, dd,16.0, 7.5)
20	2.31 (1H, m)	2.27 (1H, m)	2.20 (1H, m)	2.16 (1H, m)	2.25 (1H, m)
21	3.87 (1H, dd, 10.0, 1.0)	3.80 (1H, brd, 9.0)	3.70 (1H, d, 9.0)	3.73 (1H, brd, 8.5)	3.78 (1H, d, 9.0)
22	1.74 (1H, m)	1.80 (1H, m)	1.75 (1H, m)	ca.1.70 (1H, m)[*1]	1.80 (1H, m)
23	3.08 (1H, dd, 10.5, 2.0)	3.21 (1H, dd, 9.0,1.5)	3.21 (1H, dd, 9.0, 1.5)	3.16 (1H, brd, 9.0)	3.20 (1H, dd, 9.0, 1.5)
24	1.48 (1H, m)	1.65 (1H, m)	1.64 (1H, m)[*1]	1.64 (1H, m)	1.66 (1H, m)
25	5.16 (1H, d, 10.5)	4.97 (1H, d,10.5)	4.93 (1H, d,10.5)	4.92 (1H, d,10.5)	4.95 (1H, d,10.5)
26	1.24 (1H, m)	1.17 (1H, m)	1.21 (1H, m)	1.19 (1H, m)	1.20 (1H, m)
27	3.38 (1H, d, 8.0)	3.30 (1H, d, ca.8.0)[*1]	ca. 3.3 (1H)[*1]	ca. 3.3 (1H)[*1]	ca. 3.31 (1H)[*1]
28	5.07 (1H, dd,12.7, 8.0)	5.11 (1H, dd,12.5, 8.0)	5.11 (1H, dd,12.5, 8.0)	5.10 (1H, dd,12.5, 8.0)	5.11 (1H, dd,13.0, 8.0)
29	6.26 (1H, d,12.7)	6.24 (1H, d, 12.5)	6.23 (1H, d, 12.5)	6.23 (1H, d, 12.5)	6.23 (1H, d, 13.0)
30	2.02 (3H, s)	2.01 (3H, s)[*2]	2.04 (3H, s)	2.01 (3H, brs)	2.03 (3H, brs)
31	0.93 (3H, d, 7.0)	0.94 (3H, d, 7.0)	0.91 (3H, d, 7.0)	0.91 (3H, d, 6.5)	0.95 (3H, d, 7.0)
32	0.99 (3H, d, 7.0)	1.01 (3H, d, 7.0)	0.94 (3H, d, 7.0)	0.94 (3H, d, 6.5)	1.00 (3H, d, 7.0)
33	0.61 (3H, d, 7.0)	0.61 (3H, d, 7.0)	0.61 (3H, d, 7.0)	0.54 (3H, d, 6.5)	0.60 (3H, d, 7.0)
34	-0.21 (3H, d, 7.0)	-0.05 (3H, d,7.0)	0.01 (3H, d, 7.0)	-0.01 (3H, d, 6.5)	-0.01 (3H, d, 7.0)
36	2.02 (3H, s)	2.02 (3H, s)[*2]	2.02 (3H, s)	2.03 (3H, s)	2.02 (3H, s)
37	3.00 (3H, s)	3.00 (3H, s)	3.01 (3H, s)	3.01 (3H, s)	3.01 (3H, s)
N-CH_3	2.78 (3H, s)	2.60 (3H, s)	2.30 (3H, s)	2.65 (3H, s)	ca. 2.65 (3H, s)[*1]
PhCH=	8.32 (1H, s)	8.24 (1H, s)	8.15 (1H, s)	8.24 (1H, s)	8.21 (1H, s)
CH_2N	3.30 (4H, brm)[*1]	3.26 (4H, brm)	3.16 (2H, brm)	ca.3.3 (4H, brm)[*1]	3.25 (4H, brm)
			3.08 (2H, brm)		
	3.18 (4H, brm)	2.95 (4H, brm)	2.60 (2H, brm)	3.03 (4H, brm)[*1]	2.87 (4H, brm)
			2.55 (2H, brm)		
1'	-----	5.22 (1H, d, 4.5)	5.18 (1H, d, 4.5)	5.17 (1H, brd, ca.3.0)	5.19 (1H, d, 4.0)
2'	-----	3.93 (1H, dd, 5.5, 4.5)	4.07 (1H, dd, 5.5, 4.5)	4.06 (1H, m)	4.04 (1H, m)
3'	-----	3.88 (1H, dd, 5.5, 2.0)	ca.4.12 (1H, m)[*1]	4.03 (1H, m)	4.03 (1H, m)
4'	-----	4.00 (1H, m)	ca.4.12 (1H, m)[*1]	4.15 (1H, m)	4.12 (1H, m)
5'	-----	3.51 (2H, d, 4.0)	3.99 (1H, m)	3.99 (1H, m)	3.87 (1H, m)
			3.85 (1H, m)	3.90 (1H, m)	3.74 (1H, m)
1"	-----	-----	6.08 (1H, d, 5.5)	6.09 (1H, d, 5.5)	
2"	-----	-----	4.60 (1H, dd, 5.5, 4.5)	4.63 (1H, dd, 5.5, 4.5)	
3"	-----	-----	4.45 (1H, dd, 4.5, 4.0)	4.45 (1H, dd, 4.5, 3.5)	
4"	-----	-----	4.23 (1H, brm)	4.22 (1H, m)[*1]	
5"	-----	-----	4.20 (2H, brm)	4.22 (2H, m)[*1]	
2"'	-----	-----	8.17 (1H, s)	8.19 (1H, s)	
8"'	-----	-----	8.54 (1H, s)	8.58 (1H, s)	

*1 Overlapping with other signals.

*2 Assignments may be interchanged.

Abbreviations s: singlet, d: doublet, m: multiplet, br: broad

Table 3. ^{13}C NMR chemical shifts (δ, ppm) of rifampicin (**1**), RIP-Mb (**2**), RIP-TAs (**3**) and RIP-TAp (**5**) in CD_3OD.

Reference: methanol, δ=49.0 ppm.

Carbon	1[*6]	2[*13]	3	5	Carbon	1[*6]	2[*13]	3	5
1-10	184.0	184.8	185.9	185.4	29	144.7	144.7	144.5	144.6
	175.8	174.8	174.5	174.7	30	20.8	20.7	20.9	20.8
	149.3	149.2	149.1	149.4	31	18.2	18.3	18.4	18.3
	147.9	147.5	147.0	147.3	32	11.0	11.7	11.7	11.8
	119.7[*2]	119.5	119.1	119.3	33	9.4	10.2	10.3	10.2
	118.2	118.4	117.9	118.2	34	9.7	9.7	9.7	9.7
	116.1	116.5	116.9	116.6	35	172.4	172.5	172.5	172.6
	116.0	116.0	115.9	116.0	36	20.8	21.0	21.1	21.1
	105.0	104.6	104.1	104.4	37	56.7	56.7	56.7	56.7
	101.9	101.5	101.0	101.2	NCH_3	43.7	44.6	45.9	44.8
11	189.0	188.2	187.4	187.7	PhCH=	138.8	137.7	135.4	137.5
12	110.6	110.4	110.3	110.4	CH_2N	53.2	53.8	55.2	53.8
13	22.4	22.3	22.3	22.3		49.5[*1]	50.1	51.4	50.1
14	7.5	7.5	7.5	7.5	1'		105.1	104.9	104.9
15	171.1	170.6	170.2	170.4	2'		73.2	72.4	72.7
16	133.1	133.3	134.3	133.7	3'		71.7	71.6	71.8
17	134.8	134.8	133.8	134.3	4'		86.7	85.1[*3]	85.4[*5]
18	129.0	129.0	128.2	128.7	5'		63.5	66.8[*4]	66.2[*6]
19	140.7	141.1	140.3	140.8	1"			89.2	
20	39.1	39.4	40.3	39.8	2"			76.4	
21	75.2	75.6	73.8	74.7	3"			71.8	
22	34.4	35.0	35.2	35.1	4"			85.5[*3]	
23	78.2	87.9	86.8	87.4	5"			66.3[*4]	
24	39.4	39.6	39.3	39.4	2"'			153.8	
25	75.6	75.3	75.4	75.5	4"'			150.7	
26	41.7	42.3	42.3	42.2	5"'			120.1	
27	78.5	78.5	78.6	78.6	6"'			157.3	
28	120.1[*2]	120.0	119.4	119.6	8"'			141.3	

*1 Overlapping with other signals.

*2 Assignments may be interchanged.

*3 $J_{C\text{-}O\text{-}P}$ = 9.3 Hz

*4 $J_{C\text{-}O\text{-}P}$ = 3.7 Hz

*5 $J_{C\text{-}O\text{-}P}$ = 8.8 Hz

*6 $J_{C\text{-}O\text{-}P}$ = 3.2 Hz

9.3 Hz and that of the latter two carbons was 3.7 Hz.[19] The H-5′ signals of RIP-TAs (**3**) at δ_H 3.85 and 3.99 ppm were shifted to lower field relative to those of RIP-Mb (**2**) (δ_H 3.51 ppm)[13] by phosphorylation.[6,20] The signals due to the other protons and carbons in the spectra of RIP-TAs (**3**) were similar to those of RIP-Mb (**2**), indicating that the rest of the structure was unchanged. The glycosylation site was confirmed by a PFG-HMBC experiment, which revealed correlations of H-23 with C-1′, and H-1′ with C-23. The broad band proton-decoupled ^{31}P-NMR spectrum of RIP-TAs (**3**) showed signals at δ_P −8.88 and −8.89 ppm in an AB spin system due to the P-O-P unit of diphosphate

($J_{P\text{-}O\text{-}P}$=18.3 Hz).[21] Consequently, the structure of RIP-TAs was determined to be as shown in Figure 1.

The molecular weight and molecular formula of RIP-TAf (**4**) were the same as those of RIP-TAs (**3**), and the ^{1}H NMR signal pattern of **4** was similar to that of **3** (Table 2).[17] From the following data, it was determined that RIP-TAs (**3**) is a sodium salt and RIP-TAf (**4**) is the free form of **3**. Compared with RIP-TAs (**3**), RIP-TAf (**4**) had fewer sodium adduct ion peaks in the positive and negative ion FAB MS spectra (Table 1). Compounds **3** and **4** had the same Rf value on TLC developed with an NaCl-containing solvent. They also had the same retention time on HPLC with TFA-containing solvent (Experimental). In the purification of the conversion products of rifampicin with *E. coli* #49 homogenates by HPLC with a TFA-containing solvent, only RIP-TAf (**4**) was obtained. ADP-ribosylation of rifampicin (**1**) with *E. coli* #49 homogenates afforded RIP-TAs (**3**) and RIP-TAf (**4**) in good yield (about 72%).

The structure of RIP-TAp (**5**) was determined by comparison of the FAB MS and NMR data with those of RIP-Mb (**2**) and RIP-TAs (**3**) (Tables 1~3). The molecular formula of RIP-TAp (**5**) was determined to be $C_{48}H_{67}N_4O_{19}P$ (MW 1034). The formula is consistent with a mono-phosphorylated RIP-Mb. The presence of a ribose-5′-phosphate moiety in RIP-TAp (**5**) was indicated by the ^{13}C NMR signals at δ_C 104.9 (C-1′), 72.7 (C-2′), 71.8 (C-3′), 85.4 (C-4′) and 66.2 (C-5′) ppm, and ^{1}H NMR signals at δ_H 5.19 (H-1′), 4.04 (H-2′), 4.03 (H-3′), 4.12 (H-4′), 3.87 and 3.74 (H-5′) ppm. The $J_{C\text{-}O\text{-}P}$ values of C-4′ and C-5′ were 8.8 and 3.2 Hz, respectively. These data are similar to those of RIP-TAs (**3**). The glycosylation site was confirmed by a PFG-HMBC experiment, which demonstrated a correlation of H-23 with C-1′. The signals due to other protons and carbons in the spectra of RIP-TAp (**5**) and RIP-Mb (**2**) were similar, indicating that the remaining parts of the two structures are identical. Thus, the structure of RIP-TAp (**5**) was determined to be the 5′-phosphate of RIP-Mb (Figure 1). RIP-TAp (**5**) was unstable, and gradually decomposed in CD_3OD solution in an NMR tube.

The ^{13}C NMR chemical shifts of the ribose moiety (C-1′~C-5′) of RIP-Mb (**2**), RIP-TAs (**3**), and RIP-TAp (**5**) indicated that the stereochemistry at C-1′ of these compounds is the same.

References

1) MAGGI, N.; C. R. PASQUALUCCI, R. BALLOTTA & P. SENSI: Rifampicin: A new orally active rifamycin. Chemotherapia 11: 285~292, 1966
2) FURESZ, S.: Chemical and biological properties of rifampicin. Antibiot. Chemother. 16: 316~351, 1970
3) LANCINI, G. & W. ZANICHELLI: Structure-activity relationships in rifamycins. *In* Structure-Activity Relationships among the Semisynthetic Antibiotics. *Ed.*, D. PERLMAN, pp. 531~600, Academic Press, 1977
4) WILLIAMS, D. L.; C. WAGUESPACK, K. EISENACH, J. T. CRAWFORD, F. PORTAELS, M. SALFINGER, C. M. NOLAN, C. ABE, V. STICHT-GROH & T. P. GILLIS: Characterization of rifampin resistance in pathogenic mycobacteria. Antimicrob. Agent Chemother. 38: 2380~2386, 1994
5) YAZAWA, K.; Y. MIKAMI, A. MAEDA, M. AKAO, N. MORISAKI & S. IWASAKI: Inactivation of rifampin by *Nocardia brasiliensis*. Antimicrob. Agents Chemother. 37: 1313~1317, 1993
6) MORISAKI, N.; S. IWASAKI, K. YAZAWA, Y. MIKAMI & A. MAEDA: Inactivated products of rifampicin by pathogenic *Nocardia* spp.: Structures of glycosylated and phosphorylated metabolites of rifampicin and 3-formylrifamycin SV. J. Antibiotics 46: 1605~1610, 1993
7) YAZAWA, K.; Y. MIKAMI, A. MAEDA, N. MORISAKI & S. IWASAKI: Phosphorylative inactivation of rifampicin by *Nocardia otitidiscaviarum*. J. Antimicrob. Chemother. 33: 1127~1135, 1994
8) TANAKA, Y.; K. YAZAWA, E. R. DABBS, K. NISHIKAWA, H. KOMAKI, Y. MIKAMI, M. MIYAZI, N. MORISAKI & S. IWASAKI: Different rifampicin inactivation mechanisms in *Nocardia* and related taxa. Microbiol. Immunol. 40: 1~4, 1996
9) DABBS, E. R.; K. YAZAWA, Y. TANAKA, Y. MIKAMI, M. MIYAJI, S. J. ANDERSEN, N. MORISAKI, S. IWASAKI, O. SHIDA, H. TAKAGI & K. KADOWAKI: Rifampicin inactivation by *Bacillus* species. J. Antibiotics 48: 815~819, 1995
10) DABBS, E. R.: Rifampicin inactivation by *Rhodococcus* and *Mycobacterium* species. FEMS Microbiol. Lett. 44: 395~399, 1987
11) ANDERSEN, S. J. & E. R. DABBS: Cloning of nocardioform DNA conferring the ability to inactivate rifampicin. FEMS Microbiol. Lett. 79: 247~250, 1991
12) DABBS, E. R.; K. YAZAWA, Y. MIKAMI, M. MIYAJI, N. MORISAKI, S. IWASAKI & K. FURIHATA: Ribosylation by mycobacterial strains as a new mechanism of rifampin inactivation. Antimicrob. Agents Chemother. 39: 1007~1009, 1995
13) MORISAKI, N.; H. KOBAYASHI, S. IWASAKI, K. FURIHATA, E. R. DABBS, K. YAZAWA & Y. MIKAMI: Structure determination of ribosylated rifampicin and its derivative: New inactivated metabolites of rifampicin by micobacterial strains. J. Antibiotics 48: 1299~1303, 1995
14) QUAN, S.; H. VENTER & E. R. DABBS: Ribosylative inactivation of rifampin by *Mycobacterium smegmatis* is a principal contributor to its low susceptibility to this antibiotic. Antimicrob. Agents Chemother. 41: 2456~2460, 1997
15) QUAN, S.; T. IMAI, Y. MIKAMI, K. YAZAWA, E. R. DABBS, N. MORISAKI, S. IWASAKI, Y. HASHIMOTO & K. FURIHATA: ADP-ribosylation as an intermediate step in inactivation of rifampin by a mycobacterial gene. Antimicrob. Agents Chemother. 43: 181~184, 1999
16) IMAI, T.; K. WATANABE, Y. MIKAMI, K. YAZAWA, A. ANDO, Y. NAGATA, N. MORISAKI, Y. HASHIMOTO, K. FURIHATA & E. R. DABBS: Identification and

characterization of a new intermediate in the ribosylative inactivation pathway of rifampin by *Mycobacterium smegmatis*. Microbial Drug Resistance 5: 259~264, 1999

17) ^{13}C NMR patterns of RIP-TAs (**3**) and RIP-TAf (**4**) in CD_3OD were similar, but because **4** was not sufficiently soluble in the solvent and was unstable, complete assignment of the ^{13}C NMR signals of **4** could not be carried out. ^{13}C NMR signals of **3** and **4** in D_2O were also similar.

18) BREITMAIER, E. & W. VOELTER: A ^{13}C nuclear-magnetic-resonance study of the enzyme cofactor flavin-adenine dinucleotide. Eur. J. Biochem. 31: 234~238, 1972

19) RAGG, E.; L. SCAGLIONI, R. MONDELLI, I. CARELLI, A. CASINI & S. TORTORELLA: ^{1}H-, ^{13}C-, ^{31}P-NMR studies and conformational analysis of $NADP^+$, NADP coenzymes and of dimers from electrochemical reduction of $NADP^+$. Biochim. Biophys. Acta 1076: 49~60, 1991

20) MORISAKI, N.; S. IWASAKI, K. FURIHATA, K. YAZAWA & Y. MIKAMI: Structural elucidation of rokitamycin, midecamycin and erythromycin metabolites formed by pathogenic Nocardia. Magn. Reson. Chem. 33: 481~389, 1995

21) NONAKA, Y.; S. FUJII & T. YAMANO: Phosphorus-31 nuclear magnetic resonance and electronic spectroscopic studies of adrenodoxin reductase and its binary complex with $NADP^+$. J. Biochem. 97: 1263~1271, 1985